Control strategy of a pedal rehabilitation robot based on admittance control*

Yue Jing[1,2,3], Jinhua She[4,*], Feng Wang[1,2,3], Juan Zhao[1,2,3], and Seiichi Kawata[1,2,3]

[1] School of Automation, China University of Geosciences, Wuhan 430074, China
[2] Hubei Key Laboratory of Advanced Control and Intelligent Automation for Complex Systems, Wuhan, 430074, China
[3] Engineering Research Center of Intelligent Technology for Geo-Exploration, Ministry of Education, Wuhan 430074,China
[4] School of Engineering, Tokyo University of Technology, Hachioji, Tokyo 192-0982, Japan
2865494978@qq.com, {wangfeng, zhaojuan0859, skawata}@cug.edu.cn, she@stf.teu.ac.jp

Abstract. In recent years, Control Strategies for lower limb rehabilitation robots has attracted more and more attention. To address the abnormal mutant force in training, a rehabilitation robot admittance control strategy with a force observation threshold was designed in this paper. We developed a admittance controller and analyzed its stability from the perspective of discrete system. Activation of the admittance control was achieved by added a force observation threshold to respond to excessive mutant force. We constructed a pedal rehabilitation robot simulation platform by integrating MATLAB/Simulink and SolidWorks. The simulation results demonstrate that our method is effective in achieving training compliance and security.

Keywords: Lower limb rehabilitation robot · Admittance control · Compliance.

1 Introduction

Many people suffer from physical impairment caused by neurological injuries and diseases. Stroke is one of the leading causes of lower limb disability [1]. Rehabilitation training is physically demanding, and the number of rehabilitation

* This work was supported in part by the National Natural Science Foundation of China under Grants 62106240 and 52275018; the Natural Science Foundation of Hubei Province, China, under Grant 2020CFA031; China Postdoctoral Science Foundation under Grant 2022M722943; the 111 Project under Grant B17040; the "CUG Scholar" Scientific Research Funds at China University of Geosciences (Wuhan) under Project No.2022029; the Fundamental Research Funds for the Central Universities, China University of Geosciences (Wuhan) under Project No.CUG240635; and JSPS (Japan Society for the Promotion of Science) KAKENHI under Grants 22H03998 and 23K25252.

physicians is low [2]. Thus, the lower limb rehabilitation robot has become a hot topic in robotic fields.

There are basically two types of training strategies: active and passive. The active strategy considers the patient's motor intention and is suitable for patients with some motor ability in the middle and late stages of rehabilitation.The passive strategy is mainly used in the early stages of rehabilitation training and trains patients with weak muscles to follow a specific trajectory provided by the physician [3]. The patient's training is accompanied by abnormal mutant forces from time to time. The lack of compliance usually harms the patient's mindset and the effectiveness of the rehabilitation training, even results in secondary injuries [4].

To achieve the compliance in training, control strategies such as impedance control and admittance control play a key role in the design of controllers [5]. Both of which essentially dynamically regulate the force-position relationship between the robot end and the patient.

Stefano et al. developed a hierarchical control architecture for an upper-limb exoskeleton based on impedance control. It makes the exoskeleton work smoothly and compliantly when affected by forces generated by the user or from external [6]. Zhang et al. developed an adaptive admittance control method. It measures the torque of the ankle in real time and adaptively modifies the preset trajectory, thus improving the safety of active rehabilitation training [7]. Zhou et al. designed a spatiotemporal compliance control strategy for a new self-designed wearable lower limb rehabilitation robot (WLLRR), allowing the users to regulate the spatiotemporal characteristics of their motion [8]. Kou et al. developed a variable conductor control strategy to adapt to different patients by adjusting the conductor parameters, thus improving the wearing comfort of patients and the suppleness of training[9].

At present, the study of compliance is often incorporated into active training strategies in the middle and late stages of rehabilitation. However, compliance and safety are not adequately studied in the early stage of the passive training.

This paper developed a control strategy for the pedal rehabilitation robot based on admittance control. We first modeled the dynamics of the pedal rehabilitation robot. Then, we designed a discrete admittance controller and performed a stability analysis of the discrete system.We set the force observation threshold to complete the flexible switching between PID control and admittance control. Lastly, we constructed a robot simulation experimental platform by integrating MATLAB/Simulink and SolidWorks. This was utilized to verify the robot's horizontal plane linear trajectory motion and three-dimensional space circular trajectory motion. The experimental results validated the effectiveness of the control strategy.

2 Robot System Dynamics Model

To simplify the dynamics model, it is assumed that there is no relative movement between the human body and the robot, so that the two are considered as one en-

Fig. 1. SolidWorks model of the pedal rehabilitation robot

tity. A four-degree-of-freedom pedal rehabilitation robot model was constructed by using SolidWorks software (Fig. 1). This model considers the sagittal plane and the horizontal plane of lower limb movement, which can help to achieve a more multidirectional trajectory planning. The Lagrangian function is a mathematical model that describes the relationship between kinetic and potential energy within a system. It does not require the consideration of internal forces between systems, which can simplify the mathematical model [10,11]. Therefore, the Lagrangian method was chosen for the dynamics modelling.

The three-dimensional Cartesian coordinate system is established with point A as the origin (Fig. 2). A, B and C correspond to the centres of rotation at the hip, knee and ankle joints of the robot. $\theta_i(i = 1, 2, 3)$ denotes the angle of each joint in the sagittal plane, and θ_4 denotes the angle of rotation on the horizontal plane for the hip joint. $l_i(i = 1, 2, 3)$ denotes the length of each link, $m_i(i = 1, 2, 3)$ denotes the mass of each link, $r_i(i = 1, 2, 3)$ denotes the distance from the centre of rotation to the centre of mass $c_i(i = 1, 2, 3)$ of each link, and $I_i(i = 1, 2, 3)$ denotes the moment of inertia of each link about its centre of mass.

The positional coordinates of the centre of mass of each link are calculated as follows:

$$\begin{cases} x_{c1} = r_1 \cos\theta_1 \sin\theta_4 \\ y_{c1} = r_1 \cos\theta_1 \cos\theta_4 \\ z_{c1} = r_1 \sin\theta_1 \\ x_{c2} = (l_1 \cos\theta_1 + r_2 \cos(\theta_1 - \theta_2)) \sin\theta_4 \\ y_{c2} = (l_1 \cos\theta_1 + r_2 \cos(\theta_1 - \theta_2)) \cos\theta_4 \\ z_{c2} = l_1 \sin\theta_1 + r_2 \sin(\theta_1 - \theta_2) \\ x_{c2} = (l_1 \cos\theta_1 + r_2 \cos(\theta_1 - \theta_2) + r_3 \cos(\theta_1 - \theta_2 - \theta_3)) \sin\theta_4 \\ y_{c2} = (l_1 \cos\theta_1 + l_2 \cos(\theta_1 - \theta_2) + r_3 \cos(\theta_1 - \theta_2 - \theta_3)) \cos\theta_4 \\ z_{c2} = l_1 \sin\theta_1 + l_2 \sin(\theta_1 - \theta_2) + r_3 \sin(\theta_1 - \theta_2 - \theta_3) \end{cases} \tag{1}$$

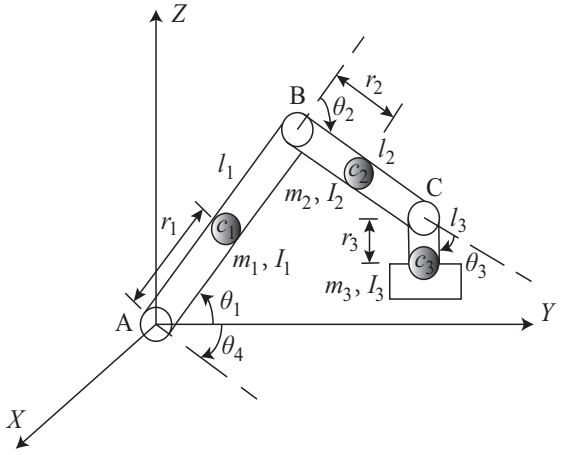

Fig. 2. Robot dynamics model

By deriving the time,the velocity of the centre of mass of each link is expressed as follows:

$$\begin{cases} \dot{x}_{ci} = \frac{dx_{ci}}{dt} \\ \dot{y}_{ci} = \frac{dy_{ci}}{dt} \\ \dot{z}_{ci} = \frac{dz_{ci}}{dt} \end{cases}, \mathrm{i} = 1, 2, 3 \tag{2}$$

In accordance with the kinetic energy theorem, the total kinetic energy of the pedal rehabilitation robot E_k is calculated as follows:

$$\begin{cases} E_{k1} = \frac{1}{2} m_1 (\dot{x}_{c1}^2 + \dot{y}_{c1}^2 + \dot{z}_{c1}^2) + \frac{1}{2} I_1 \dot{\theta}_1^2 \\ E_{k2} = \frac{1}{2} m_2 (\dot{x}_{c2}^2 + \dot{y}_{c2}^2 + \dot{z}_{c2}^2) + \frac{1}{2} I_2 (\dot{\theta}_1 - \dot{\theta}_2)^2 \\ E_{k3} = \frac{1}{2} m_3 (\dot{x}_{c3}^2 + \dot{y}_{c3}^2 + \dot{z}_{c3}^2) + \frac{1}{2} I_3 (\dot{\theta}_1 - \dot{\theta}_2 - \dot{\theta}_3)^2 \\ E_k = \sum_{i=1}^{3} E_{ki} + \frac{1}{2} (I_1 + I_2 + I_3) \dot{\theta}_4^2 \end{cases} \tag{3}$$

Subsequently, the total potential energy of the robot E_p is obtained by employing the $X - Y$ plane as the zero potential energy surface:

$$\begin{aligned} E_p = \sum_{i=1}^{3} E_{pi} = \sum_{i=1}^{3} m_i g z_{ci} = (m_1 g r_1 + m_2 g l_1 + m_3 g l_1) \sin\theta_1 + \\ (m_2 g r_2 + m_3 g l_2) r_2 \sin(\theta_1 - \theta_2) + m_3 g r_3 \sin(\theta_1 - \theta_2 - \theta_3) \end{aligned} \tag{4}$$

The construction of Lagrangian functions for the robots is as follows:

$$L = E_k - E_p \tag{5}$$

Finally, the Lagrangian dynamics equation of the robot is derived as:

$$\tau = \frac{d}{dt} \frac{\partial L}{\partial \dot{\theta}} - \frac{\partial L}{\partial \theta} \tag{6}$$

$$H(\theta)\ddot{\theta} + C(\theta,\dot{\theta})\dot{\theta} + G(\theta) = \tau \tag{7}$$

In practice, the simplified form of the Lagrangian kinetic equation in Eq.(7) is frequently employed , where θ is the generalized coordinates of the kinetic and potential energy of the system, $\dot{\theta}$ is the generalized velocity, and τ is the driving moment. $H(\theta)$, $C(\theta,\dot{\theta})$, and $G(\theta)$ represent inertia matrix, centrifugal and Coriolis force matrix, and gravity matrix. The torque-based control algorithm establishes the force-position relationship in joint space and Cartesian space in Eq.(8), where J is the Jacobi matrix.

$$\begin{cases} \dot{X} = J\dot{\theta} \\ \tau = J^T F \end{cases} \tag{8}$$

3 Principle

3.1 Control Strategy

During the rehabilitation training process, we use a torque sensor to detect the interaction force between the robot and the patient. And we design an admittance controller to update the robot end trajectory in real time. The tracked end trajectory is transformed into the angular changes at each joint through inverse kinematics. Excessive mutant force will make the displacement along the direction of force compliance too large, and the angular threshold function is set to limit it to a certain range(Fig.3).

The generation of abnormal mutation forces is detected by setting a force observation threshold, which activates the admittance control to achieve compliance in rehabilitation training. The active force within the threshold is small in the early stages of rehabilitation, tracking control is performed; when the interaction force is greater than the preset threshold, the admittance controller is activated to follow the trajectory movement in the direction of the force, to ensure the safety of the patient's rehabilitation by improving compliance, and when the force disappears, the rehabilitation robot returns to the original planning trajectory to continue tracking control.

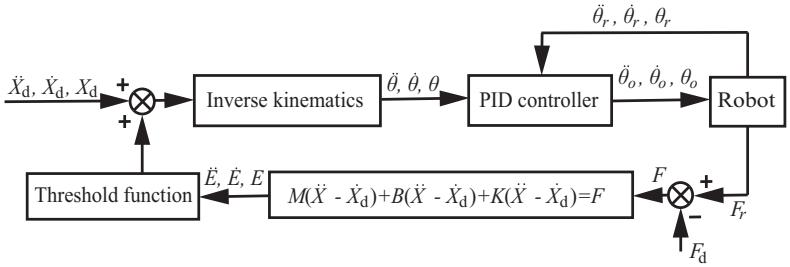

Fig. 3. Compliant control block diagram

3.2 Admittance Controller

The fundamental principle of admittance Control is to permit the patient to deviate from a predefined reference trajectory in lieu of compelling the patient to move along a fixed trajectory. The degree of deviation is contingent upon the magnitude of the torque exerted by the patient, in addition to the patient's behavioral pattern.

The control strategy equates the robot control system to a second-order physical model of "mass-damping-spring", where the inertia, damping and stiffness parameters are adjusted to achieve a dynamic relationship between the robot end-effector and the force(Fig.4).The mathematical form of admittance control is shown as follows:

$$M(\ddot{X} - \ddot{X}_d) + B(\dot{X} - \dot{X}_d) + K(X - X_d) = F \tag{9}$$

For a four-degree-of-freedom pedal rehabilitation robot, M, B and K are (4×4) positive definite symmetric matrices called inertia coefficient matrix, damping coefficient matrix, and stiffness coefficient matrix, which are decoupled in each direction. X_d is the desired position of the robot end, X is the actual position of the robot end, and F is the contact force between the robot and the patient. The robot end-effector $X - Y - Z$ is required to be decoupled in the three directions, which facilitates separate control in the three directions. Therefore, we can start by considering only the one-dimensional case by taking m, b, k, f to be the one-dimensional elements in M, B, K, F:

$$m(\ddot{x} - \ddot{x}_d) + b(\dot{x} - \dot{x}_d) + k(x - x_d) = f \tag{10}$$

When we use the admittance control algorithm applied to a real system, it can often be implemented by discretising the programming on the controller in Eq.(11). $x(nT)$ is the actual motion position of the robot end at the nth sampling cycle, $x_d(nT)$ is the desired position of the robot end at the nth sampling cycle, and T is the sampling time.

$$\begin{cases} x[(n+1)T] = x(nT) + \dot{x}(nT)T \\ \dot{x}[(n+1)T] = \dot{x}(nT) + \ddot{x}(nT)T \\ m[\ddot{x}(nT) - \ddot{x}_d(nT)] = \\ f - b[\dot{x}(nT) - \dot{x}_d(nT)] - k[x(nT) - x_d(nT)] \end{cases} \tag{11}$$

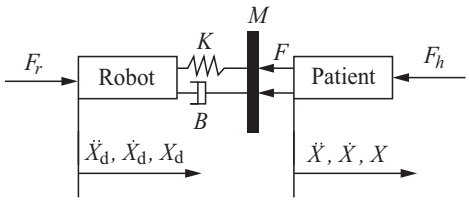

Fig. 4. Admittance control model

In the practical application of the conduction control algorithm, the original second-order continuous system is transformed into its discrete form, with the introduction of the sampling time T and the parameters m, b and k. While this transformation introduces a constraint relationship between the internal variables, it does not guarantee that the discrete control system is always stable. To verify the stability of this discrete system, its state variables and output variables are taken as follows:

$$\begin{cases} x_1(n) = x(n) \\ x_2(n) = \dot{x}_1(n) = \dot{x}(n) \\ y(n) = x_1(n) \end{cases} \tag{12}$$

The variables in Eq. (11) are converted as follows:

$$\begin{cases} x_1(n+1) = x_1(n) + x_2(n)T \\ x_2(n+1) = -\frac{kT}{m}x_1(n) + (1 - \frac{bT}{m})x_2(n) + u(n) \\ y(n) = x_1(n) \end{cases} \tag{13}$$

In most cases, $u(n)$ is treated as a control quantity:

$$u(n) = \ddot{x}_d(n)T + \frac{1}{m}[f + b\dot{x}_d(n) + kx_d(n)]T \tag{14}$$

The state space model of this discrete system is described as:

$$\begin{cases} x(n+1) = \begin{bmatrix} 1 & T \\ -\frac{kT}{m} & 1 - \frac{bT}{m} \end{bmatrix} \begin{bmatrix} x_1(n) \\ x_2(n) \end{bmatrix} + u(n) \\ y(n) = \begin{bmatrix} 1 & 0 \end{bmatrix} \begin{bmatrix} x_1(n) \\ x_2(n) \end{bmatrix} \end{cases} \tag{15}$$

The stability of this system is generally determined by the coefficient matrix:

$$G = \begin{bmatrix} 1 & T \\ -\frac{kT}{m} & 1 - \frac{bT}{m} \end{bmatrix} \tag{16}$$

The Jury stability criterion is applied directly in the Z-domain and is particularly suitable for the stability analysis of second-order discrete systems. Next, we use this criterion for the stability analysis of the system. This is achieved by setting the characteristic equation of the n order discrete system as follows:

$$F(z) = a_n z^n + a_{n-1} z^{n-1} + \cdots + a_1 z + a_0 = 0 (a_n > 0) \tag{17}$$

According to the coefficients of the characteristic equation, the system satisfies the stability conditions as follows:

$$\begin{cases} a2 + a1 + a0 > 0 \\ a2 - a1 + a0 > 0 \\ a2 > |a0| \end{cases} \tag{18}$$

For a second-order discrete derivative control system, the corresponding characteristic equation is is described as:

$$F(z) = |zI - G| = z^2 + (\frac{bT}{m} - 2)z + 1 - \frac{bT}{m} + \frac{kT^2}{m} = 0 \tag{19}$$

In order to stabilise the system, the coefficients in Eq. (19) are transferred to Eq. (18) for calculation:

$$\begin{cases} 1 + (\frac{bT}{m} - 2) + 1 - \frac{bT}{m} + \frac{kT^2}{m} > 0 \\ 1 - (\frac{bT}{m} - 2) + 1 - \frac{bT}{m} + \frac{kT^2}{m} > 0 \\ 1 > \left|1 - \frac{bT}{m} + \frac{kT^2}{m}\right| \end{cases} \tag{20}$$

The condition for the stability of this discrete system is solved as:

$$\begin{cases} b^2 \geq 4mk, 0 < \mathrm{T} < \frac{b - \sqrt{b^2 - 4mk}}{k} \\ b^2 < 4mk, 0 < \mathrm{T} < \frac{b}{k} \end{cases} \tag{21}$$

Under the premise of satisfying the stability of the system, we can achieve different dynamic performances by selecting appropriate parameters. Therefore, the parameters are test-fitted to meet different degrees of rehabilitation training intensity and task requirements.

4 Simulation

4.1 The horizontal plane linear trajectory motion

In order to verify the compliance achieved by the admittance controller in rehabilitation training, a sinusoidal signal and a random noise signal are introduced to represent the active force of the patient in training, and the addition of an extra force signal is regarded as the patient's mutation force, so that the simulated human-computer interaction force shown by black line in Fig. 5 is obtained. The red line in Fig. 5 is the upper and lower limits of the threshold value set by the Compliant control.

Figure 6 shows the trajectory changes in the y-direction (one-dimensional): the horizontal reference trajectory Y_d is the blue line, the actual running trajectory Y_r is shown as the red line, and the running trajectory after softening Y_{rr} is shown as the black line.When the patient's active force exceeds the preset threshold, the robot is able to instantly control the patient's compliance and move in the direction of the force, thereby effectively avoiding secondary injury to the patient. Once the abnormal force has dissipated, the robot returns to its original trajectory, resuming passive rehabilitation training. Furthermore, the trajectory of the robot following softening indicates that it remains within the safety range, thereby effectively avoiding the potential harm caused by excessive range of motion.

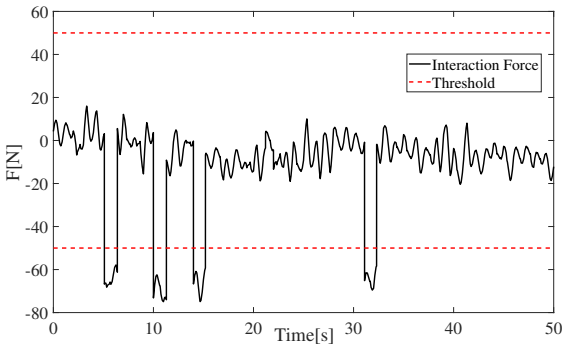

Fig. 5. Human-robot interaction force

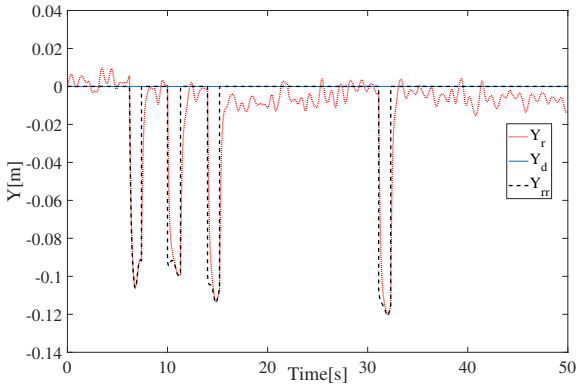

Fig. 6. Change in trajectory in the Y-direction

4.2 The three-dimensional space circular trajectory motion

A simulation platform for the pedal rehabilitation robot was constructed by integrating MATLAB/Simulink and SolidWorks software (Fig. 7):The utilisation of the SimMechanics module based on Simulink enables the modelling and 3D analysis of mechanical systems. The pedal rehabilitation robot constructed in SolidWorks was imported into this module, and the requisite components, including rotary joints and PID control components, were incorporated to create a standalone robotics experimental system.

We designed a reference trajectory X_d for the robot end to move in a circle in the $Y-Z$ plane of the Cartesian coordinate system from a relative initial position, and observed the trajectory tracking when the patient's active force is too large and exceeds the threshold value. X_r represents the actual tracking trajectory following the implementation of the compliant control(Fig. 8). The

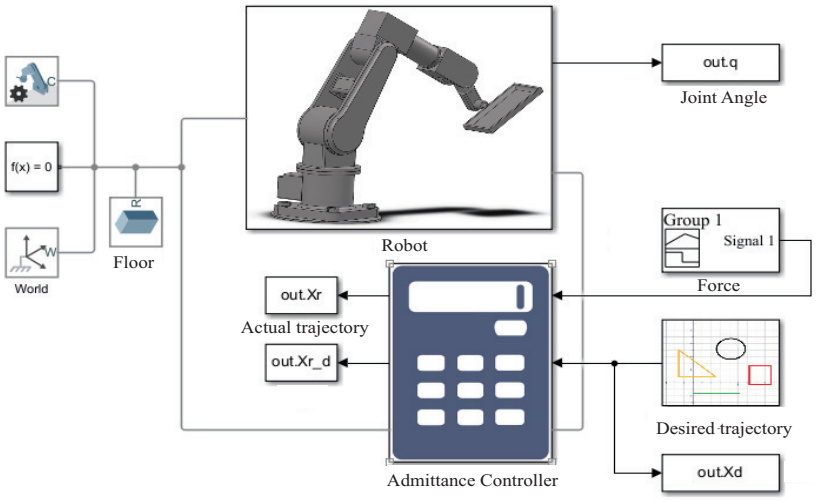

Fig. 7. Simulation platform for rehabilitation robot based on admittance controller

robot end is displaced from the reference trajectory due to the patient's active force, and then returns to the reference trajectory motion when the active force dissipates. Figure 9 illustrates the angular displacement of each joint, demonstrating that each joint is capable of compensating for the patient's active force by modifying its current trajectory. The trajectory tracking results of the actual operation meet the expectations and validates the effectiveness of the compliant control strategy.

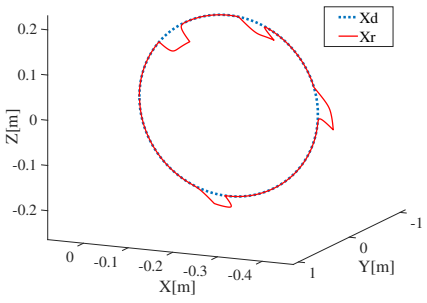

Fig. 8. Desired and actual trajectories of the robot end in Cartesian space

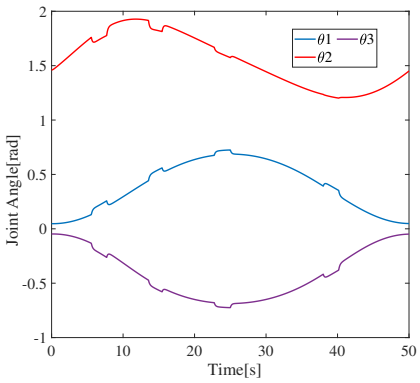

Fig. 9. Desired and actual trajectories of the robot end in Cartesian space

5 Conclusion

The paper designed an admittance control strategy with a force observation threshold as a solution to the problem of passive training compliance in the early stages of rehabilitation. A simulation experiment platform for the pedal rehabilitation robot was constructed. The experimental results show that it immediately activates the admittance controller when excessive abnormal mutation force is detected. When the force disappears, it returns to the original trajectory tracking process, demonstrating that the control strategy achieves compliance and flexibility in passive training. Furthermore, the control strategy designed in this paper and the architecture of the simulation and experimental system can be combined with some adaptive control algorithms and intelligent control algorithms to achieve better control effects. This will be the next step to be completed.

References

1. Wang, L., Brief report on stroke prevention and prevention and treatment in China. Mechatronics **20**(1), 783–793 (2023).
2. Wu, Q., Chen, Y., Variable admittance time-delay control of an upper limb rehabilitation robot based on human stiffness estimation. Mechatronics **90**, 102935 (2023).
3. Lv, X., Yang, Z., Jiang, F., Han, J., Passive training control of horizontal lower limbs rehabilitative robot. Machinery Design and Manufacture **(**4), 244–247 (2019).
4. Wang, W., Liang, X., Liu, S., Lin, T., Zhang, P., Zhen, L., Wang, J., and Hou, Z., Drivable space of rehabilitation robot for physical human-robot interaction: definition and an expanding method. IEEE Transactions on Robotics **39**(2), 343–356 (2023).
5. Arnold, J., and Lee, H., Variable impedance control for pHRI:impact on stability, agility, and human effort in controlling a wearable ankle robot. IEEE Robotics and Automation Letters **6**(2), 2429–2439 (2021).

6. Dalla Gasperina, S., Gandolla, M., Longatelli, V., Panzenbeck, M., Luciani, B., Braghin, F., and Pedrocchi, A.L., AGREE: A compliant-controlled upper-limb exoskeleton for physical rehabilitation of neurological patients. IEEE Transactions on Medical Robotics and Bionics **5**(1), 143–154 (2023).
7. Zhang, M., Xie, S., Li, X., Zhu, G., Meng, W., Huang, X., and Veale, A.J., Adaptive patient-cooperative control of a Compliant Ankle Rehabilitation Robot (CARR) with enhanced training safety. IEEE Transactions on Industrial Electronics **65**(2), 1398–1407 (2018).
8. Shen, H., Liu, X., and Liu, K., Spatiotemporal compliance control for a wearable lower limb rehabilitation robot. IEEE Transactions on Biomedical Engineering **70**(6), 1858–1868 (2023).
9. Kou, J., Wang, Y., Chen, Z., Shi, Y., Guo, Q., and Xu, M., Flexible assistance strategy of lower limb rehabilitation exoskeleton based on admittance model. Science China(Technological Sciences) **67**(3), 823–834 (2024).
10. Chen, Z., Yi, T., Pan, H., Zhao, S., A three degree of freedom parallel ankle rehabilitation mechanism. Journal of Mechanical Engineering **56**(21), 70–78 (2020).
11. Huang, Z., Research on modeling and motion simulation of rehabilitation robot based on ADAMS. Electronic Measurement Technology **43**(9), 127–132 (2020).